2025, vol. 16, n° 4, 49-75 pages, DOI: 10.21494/ISTE.OP.2025.1342

A practical guide to analyzing discrete models

Guide pratique pour l'analyse des modèles discrets

Jose S. Cánovas

Departamento de Matemática Aplicada y Estadística, Universidad Politécnica de Cartagena,
C/ Doctor Fleming sn, 30202, Cartagena, Spain
Jose.Canovas@upct.es

ABSTRACT. In this paper, we survey valuable results to analyze discrete models frequently appearing in social and natural sciences. We review some well-known results and tools to analyze these systems, trying to make them as practical as possible so that not only mathematicians but also physicists, economists or biologists can use them to explore their models. Applying these methods requires some basic knowledge of computational tools and basic programming. The reviewed topics vary from the local stability of equilibrium points to the characterization of topological and physically observable chaos.
KEYWORDS. discrete dynamical systems, stability, periodicity, bifurcations, chaos, entropy.

1. Introduction

In the last decades, there has been a great interest in modelling some phenomena of social and natural sciences by using difference equations, that is, discrete-time models. Later, we will give some examples. Now, we will set the general framework for these models.

The hypothesis are simple, we consider a subset $X \subseteq \mathbb{R}^n$, where $n \in \mathbb{N}$, and a map $\mathbf{f} : X \to X$ which is at least continuous, but often it is C^k for some $k \in \mathbb{N} \cup \{\infty\}$. Then, the difference equation has the form

$$\mathbf{x}_{n+1} = \mathbf{f}(\mathbf{x}_n), \quad \mathbf{x}_0 \in X. \tag{1}$$

Alternatively, the pair $(X, \mathbf{f})$ is a discrete dynamical system. So, the orbit of an initial condition $\mathbf{x}_0$ is given by the sequence $\mathbf{x}_n$. The limit points of the sequence $\mathbf{x}_n$ is the ω-limit set of $\mathbf{x}_0$ under $\mathbf{f}$. The dynamics of $(X, \mathbf{f})$ is known when we can describe the asymptotic dynamics of all the possible orbits, that is, the set of all the possible ω-limit sets. However, this knowledge is quite difficult to achieve in general.

Roughly speaking, the models evolving with time can be of two types, continuous-time models given by differential equations and discrete-time ones, modeled by difference equations. The advantage of discrete-time models is that computers also work in discrete time. Then, it is pretty simple to write a computer program to simulate the evolution of the sequence $\mathbf{x}_n$ defined above. The same task for continuous time models requires a previous step of discretizing the model, adding additional errors to the computations. In contrast, analytical methods are more developed for continuous models since the theory of discrete dynamical systems is relatively new.

The above mentioned advantage of the discrete models has given rise to a plethora of models, mainly in biology and economy, but also in other branches of science. Below, we introduce some examples of discrete modeling.

- One of the most famous models was introduced by May in [45]. It is a population dynamics model given by the difference equation

  $$x_{n+1} = ax_n(1 - x_n),$$

  where $a \in (0, 4]$ and the initial conditions are taken inside the interval $[0, 1]$. The dynamics of this model have been studied by many authors (see, e.g., the survey [58]).

- Also, biological models are the Beverton-Holt model (see [9]), given by

  $$x_{n+1} = \frac{KRx_n}{K + (R - 1)x_n},$$

  where $R > 1$ and $K > 0$ and $x_n \geq 0$, and the Ricker model

  $$x_{n+1} = Ax_n e^{-x_n},$$

  where $A > 1$ and $x_n \geq 0$ (see [51]). A variation of the last model is the so-called γ-Ricker model (see [44])

  $$x_{n+1} = Ax_n^{\gamma} e^{-x_n},$$

  where the new parameter γ is greater than one.

- There exists a huge literature on discrete-time economic models (see e.g. the monograph [10] and the references [11], [25], [39] or [49]). For instance, the two last models are given by a system of two difference equations with the form

  $$\begin{cases} x_{n+1} = f(y_n), \\ y_{n+1} = g(x_n), \end{cases}$$

  where x_n and y_n are the outputs of two firms competing in a market with specific rules that produce the functions f and g, called reaction functions.

- Finally, let us mention an example from physics. In the last years, the notion of q-deformations, a notion coming from non-extensive statistical mechanics (see [59]), received the attention of several scientists (see [5, 18, 24, 37]). Roughly speaking, a q-deformed number $[x]_q$, $x \in \mathbb{R}$ is given by a one-parameter family of map ϕ_q such that $\phi_q(x) = [x]_q$ converges to x when q converges to one. A typical example is

  $$[x]_q := \frac{x}{1 + (1 - q)(1 - x)},$$

  with $q \in (-\infty, 2)$. A q-deformation of a real map f is a map f_q given by $f([x]_q)$, $x \in X$. Here, X is a suitable subinterval of the real line. When the map f is indeed a one-parameter family of maps, for instance, the logistic map $f_a(x) = ax(1 - x)$, the resulting family is $f([x]_q)$ which depends on two parameters and has a richer dynamics, included the so-called Parrondo's paradox (see, e.g., [20]), where the composition of two dynamically simple maps gives rise to a map with a complex dynamical behavior, which we will introduce in what follows.

This paper aims to provide some practical techniques for analyzing models of the type presented above. Here, the word practical means the use of computers as instruments for visualizing or simulating the model dynamics. Of course, these simulations are affected by round-off errors. So, we will present analytical results supporting the simulations when they will be available. The existence of such analytical results will imply a strong hypothesis on both X and $\mathbf{f}$, so the paper will have plenty of open problems to support analytically the obtained simulations unless otherwise stated.

Our methodology is as follows. We will introduce the techniques in the most general framework, usually illustrated with a model. From this general setting, we will move to more concrete scenarios where analytical results will support the simulations. We will differentiate between simple dynamics, given by periodic orbits, and complex dynamics, given by unpredictable or chaotic orbits.

The paper is planned to be self-contained and organized as follows. Periodic or regular motions will be analyzed in the next section, while the last section will be devoted to complex dynamics. Each section is divided into several subsections covering different topics included in that section.

2. Periodic motions

Let $(X, \mathbf{f})$ be a discrete dynamical system. For $n \in \mathbb{N}$, let $\mathbf{f}^n = \mathbf{f} \circ \mathbf{f}^{n-1}$, where $\mathbf{f}^0$ denotes the identity on X and $\mathbf{f}^1 = \mathbf{f}$. A point $\mathbf{x}_0 \in X$ is said to be periodic (of period $k \in \mathbb{N}$) if $\mathbf{f}^k(\mathbf{x}_0) = \mathbf{x}_0$ and $\mathbf{f}^i(\mathbf{x}_0) \neq \mathbf{x}_0$ for $i = 1, 2, ..., k-1$. Then, the sequence defined by the difference equation (1) is periodic of period k. Periodic points of period one are called fixed points and usually play a very important role in applied models. Note that a periodic point of period k is a fixed point for $\mathbf{f}^k$.

It is clear that the ω-limit set of a periodic orbit is the orbit itself, and hence, the dynamics are easily predictable or simple. However, it is important to know whether a periodic orbit is the ω-limit set of a sufficiently big subset $A \subseteq X$ of initial conditions. This idea will be analyzed below.

2.1. *Stability*

A fixed point $\mathbf{x}_0 \in X$ is locally stable if for any $\epsilon > 0$ there exists $\delta > 0$ such that for all $\mathbf{x} \in X$ with $||\mathbf{x} - \mathbf{x}_0|| < \delta$ we have that $||\mathbf{f}^n(\mathbf{x}) - \mathbf{x}_0|| < \epsilon$ for all $n \in \mathbb{N}$. Otherwise, the fixed point $\mathbf{x}_0$ will be called unstable. $\mathbf{x}_0$ is attracting if there exists $\delta > 0$ such that $||\mathbf{x} - \mathbf{x}_0|| < \delta$ implies $\lim_{n \to \infty} \mathbf{f}^n(\mathbf{x}) = \mathbf{x}_0$. When $\mathbf{x}_0$ is locally stable and attracting, we say that it is locally asymptotically stable, shortly LAS. We say that $\mathbf{x}_0$ is globally asymptotically stable, shortly GAS, if any orbit converges to $\mathbf{x}_0$. Obviously, GAS implies LAS, but the opposite is not true.

For $\mathbf{f}$ smooth enough, the next well-known result is quite useful to characterize LAS. Assume that $\mathbf{Jf}(\mathbf{x}_0)$ is the Jacobian matrix of $\mathbf{f}$ at $\mathbf{x}_0$, and denote $\sigma(\mathbf{Jf}(\mathbf{x}_0)) = \max\{|\lambda| : \lambda$ is an eigenvalue of $\mathbf{Jf}(\mathbf{x}_0)\}$. Then, if $\sigma(\mathbf{Jf}(\mathbf{x}_0)) < 1$, then $\mathbf{x}_0$ is LAS. If $\sigma(\mathbf{Jf}(\mathbf{x}_0)) > 1$ then $\mathbf{x}_0$ is repelling (it is not LAS). When $\sigma(\mathbf{Jf}(\mathbf{x}_0)) = 1$, it is unclear whether $\mathbf{x}_0$ is LAS or not.

Example 2.1. Let $x_{n+1} = f_a(x_n) = a x_n(1 - x_n)$ be the logistic model with $a \in (0, 4]$ and $x_n \in [0, 1]$. The fixed points of f_a are 0 and $\frac{a-1}{a} \neq 0$, when $a > 1$. As $f_a'(x) = a(1 - 2x)$, and $f_a'(0) = a$, we have that 0 is LAS for $a < 1$ and it is repelling when $a > 1$. For $a > 1$, we have that $f_a'\left(\frac{a-1}{a}\right) = 2 - a$, so that $\frac{a-1}{a}$ is LAS when $a < 3$.

When $a > 3$, we have a periodic point of order two given by

$$x_{\pm} = \frac{1 + a \pm \sqrt{(a+1)(a-3)}}{2a}.$$

Here we note that $f(x_+) = x_-$ and $f(x_-) = x_+$. As $f_a'(x_+)f_a'(x_-) = 4 + 2a - a^2$, it is straightforward to check that $|4 + 2a - a^2| < 1$ provided $a \in (3, 1 + \sqrt{6})$. So, the periodic orbit is LAS whenever $a \in (3, 1 + \sqrt{6})$. We cannot analyse the local stability of periodic orbits analytically; we must use numerical analysis since solving the equation $f_a^3(x) = x$ implies the solution of a polynomial equation of degree six.

Example 2.2. Let $x_{n+1} = f_a(x_n) = ax_n(1 - x_{n-1})$ be the delayed logistic model. Again, the fixed points of f_a are 0 and $\frac{a-1}{a} \neq 0$, when $a > 1$. Now, we introduce a new variable y_n to write the model as

$$\begin{cases} y_{n+1} = x_n, \\ x_{n+1} = ax_n(1 - x_{n-1}). \end{cases}$$

Writing $\mathbf{f}_a(y, x) = (x, ax(1 - y))$, we have that

$$\mathbf{Jf}(y, x) = \begin{pmatrix} 0 & 1 \\ -ax & a(1 - y) \end{pmatrix}.$$

The characteristic polynomial of $\mathbf{Jf}(0, 0)$ is $p(t) = t(t - a)$, so again we find that 0 is LAS when $a < 1$. For $\mathbf{Jf}\left(\frac{a-1}{a}, \frac{a-1}{a}\right)$ we have $p(t) = t^2 - t + a - 1$, with roots

$$t_\pm = \frac{1 \pm \sqrt{5 - 4a}}{2}.$$

From them, it is straightforward to check that $\frac{a-1}{a}$ is LAS when $1 < a < 2$.

LAS and GAS are equivalent notions for linear systems, but this is not the case in nonlinear models. The following section will consider this question for one-dimensional models using the Schwarzian derivative.

2.2. *The role of Schwarzian derivative in one dimension*

Let $f : X \subset \mathbb{R} \to X$ be a C^3 map with X a subinterval of the real line. For $x \in X$, the Schwarzian derivative of f is given by

$$\mathcal{S}(f)(x) = \frac{f^{(3)}(x)}{f'(x)} - \frac{3}{2}\left(\frac{f''(x)}{f'(x)}\right)^2,$$

whenever $f'(x) \neq 0$. In dynamics, the Schwarzian derivative was introduced in [53], representing an essential notion when analyzing smooth enough one-dimensional models. It is helpful in several settings to characterize LAS for non-hyperbolic fixed points, to study when LAS implies GAS and, as we will see later on, to characterize the number of Milnor attractors.

The characterization of LAS for non-hyperbolic fixed points can be divided into two cases (see [29]). Namely, if $x_0 \in X$ is a fixed point, the non-hyperbolicity implies that either $f'(x_0) = 1$ or $f'(x_0) = -1$. If $f'(x_0) = 1$, then x_0 is LAS when $f^{(k)}(x_0) = 0$ for $k = 2, ..., l - 1$, and $f^{(l)}(x_0) < 0$ with l odd. If l is even, then x_0 is semistable, which means that it attracts orbits with initial conditions in a neighborhood of the fixed point, but only for those initial conditions smaller or greater than x_0, but not both. When $f'(x_0) = -1$, then the fixed point is LAS whenever $\mathcal{S}(f)(x_0) < 0$.

Example 2.3. Let us have a look at Example 2.1. For $a = 1$, we have that $f_a'(0) = 1$. As $f_a''(x) = -2a < 0$, we have that the fixed point 0 is LAS. For $a = 3$, we have that $f_a'\left(\frac{a-1}{a}\right) = -1$. As

$$\mathcal{S}(f_a)(x) = -\frac{6}{(1-2x)^2} < 0$$

for all $x \neq 1/2$, we have that the fixed point $\frac{a-1}{a}$ is also LAS.

Now, let us move to the question of whether LAS implies GAS. We say that the map f is unimodal if there exists $c \in X$ such that $f|_{\{x \in X: x<c\}}$ is increasing and $f|_{\{x \in X: x>c\}}$ is decreasing. Obviously, c is a maximum of f. The following result can be found in [53].

Theorem 2.4. *Assume that a unimodal map f has a unique fixed point x which is LAS. If $\mathcal{S}(f)(x) < 0$, then x is GAS.*

Example 2.5. Let us consider again Example 2.1. We know that the fixed point 0 is LAS whenever $0 < a \leq 1$. Since there is not other fixed points and the Schwarzian derivative is negative, then by Theorem 2.4, we find that 0 is also GAS, that is, every orbit with initial condition in $[0, 1]$ will converge to 0. For $1 < a \leq 3$ we know that $\frac{a-1}{a}$ is the unique non-zero fixed point. Again by Theorem 2.4 we have that it is GAS in $(0, 1)$, that is any orbit with initial condition in $(0, 1)$ will converge to $\frac{a-1}{a}$. Recall that the logistic model is a population dynamics model, so for $a \leq 1$ we would have the global extinction of the population. In contrast, for $a \in (1, 3]$ the population will evolve to a stationary population. Characterizing this stationary population as GAS is an important problem in population dynamics.

Example 2.6. We consider the Berverton-Holt model

$$x_{n+1} = \frac{KRx_n}{K + (R-1)x_n},$$

where $R > 1$ and $K > 0$ and $x_n \geq 0$. The map

$$f_{K,R}(x) = \frac{KRx}{K + (R-1)x}$$

has two fixed points, namely 0 and K. As $f_{K,R}'(0) = R$, we have that 0 is LAS whenever $R < 1$, which is impossible. As $f_{K,R}'(K) = \frac{1}{R}$, we have that the fixed point K is LAS when $R > 1$. The question is whether the non-zero fixed point is also GAS. Here $\mathcal{S}(f_{K,R})(x) = 0$, so we do not have the help of the Schwarzian derivative. However, it is easy to check that the map $f_{K,R}$ is strictly increasing and such that $f_{K,R}(x) > x$ for $x \in (0, K)$ and $f_{K,R}(x) < x$ for $x \in (K, +\infty)$, and it is simple to realize that then any orbit with initial condition in $(0, +\infty)$ will converge to K.

In the examples above, it was possible to compute explicitly the fixed points. However, this computation can be a formidable task in some cases. The example below gives us some ideas on how to deal with this situation.

Example 2.7. We consider the γ-Ricker model

$$x_{n+1} = Ax_n^{\gamma} e^{-x_n},$$

where $A \geq 1$, $\gamma > 1$ and $x_n \geq 0$. The map

$$f_{A,\gamma}(x) = Ax^{\gamma} e^{-x}$$

has 0 as a fixed point. A non-zero fixed point x_0 must satisfy that

$$Ax_0^{\gamma-1}e^{-x_0} = 1,$$

but this equation cannot be solved by using elementary functions when $\gamma > 1$, although one can find them by using the so-called Lambert function [63]. Anyhow, one can find the parameter region where the non-zero fixed points exist and characterize their stability as follows. It is easy to see that

$$f'_{A,\gamma}(x) = Ax^{\gamma-1}e^{-x}(\gamma - x).$$

So, on the one hand, we have that $f'_{A,\gamma}(0) = 0$ and consequently, the fixed point 0 is always LAS. For the non-zero fixed point x_0 we have that the system

$$\begin{cases} f_{A,\gamma}(x_0) = Ax_0^{\gamma-1}e^{-x_0} = 1, \\ f'_{A,\gamma}(x_0) = Ax_0^{\gamma-1}e^{-x_0}(\gamma - x_0) = -1, \end{cases} \tag{2}$$

gives us the condition to have a derivative equal to -1, which reduces to

$$x_0 = 1 + \gamma,$$

and substituting in the first equation

$$A_{-1}(\gamma) = (1+\gamma)^2 \left(\frac{e}{1+\gamma}\right)^{\gamma+1}$$

Similarly, the system

$$\begin{cases} f_{A,\gamma}(x_0) = Ax_0^{\gamma-1}e^{-x_0} = 1, \\ f'_{A,\gamma}(x_0) = Ax_0^{\gamma-1}e^{-x_0}(\gamma - x_0) = 1, \end{cases} \tag{3}$$

gives us the condition to have a derivative equal to 1, which is

$$x_0 = \gamma - 1,$$

and proceeding as above

$$A_1(\gamma) = \left(\frac{e}{\gamma-1}\right)^{\gamma-1}.$$

As $A_1(\gamma) \leq A_{-1}(\gamma)$, Figure 1 shows the stability region of the non-zero fixed point. So, although we cannot compute explicitly the fixed points, we are able to draw the stability region in the parameter space.

2.3. *Criterion for LAS (and GAS) in higher dimension*

When the dimension of the phase space X is bigger than one, it is not a simple task to decide whether a fixed point $\mathbf{x}_0$ is LAS. Assuming $\mathbf{f}$ smooth enough, one should compute the eigenvalues of the Jacobian matrix $\mathbf{Jf}(\mathbf{x}_0)$. If the dimension of X is $m \in \mathbb{N}$, this computation must be done by solving the polynomial equation $p(t) = 0$, where $(-1)^m p(t)$ is the characteristic polynomial of $\mathbf{Jf}(\mathbf{x}_0)$. Recall that usually, the models depend on one or several parameters, so $p(t)$ also has this dependence. It is well-known that when $m \geq 5$, in general, there are no formulas for obtaining the solutions, and even when m is smaller than five, these solutions can be difficult to handle or even useless.

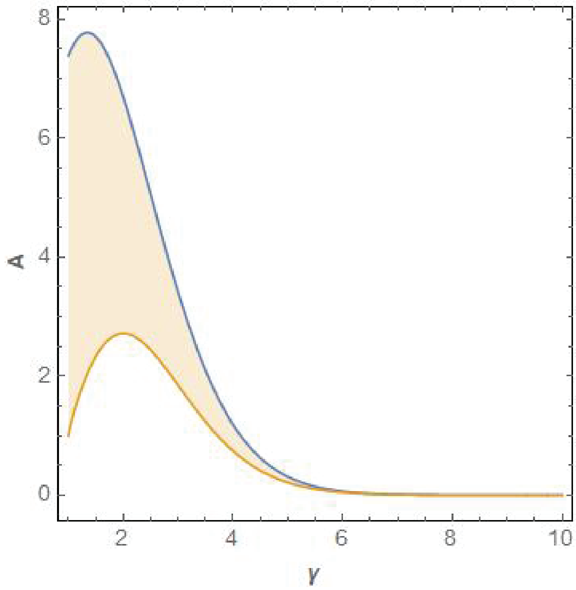

Figure 1. *We depict in shadow the stability region of the non-zero fixed point of the γ-Ricker map.*

The Jury's criterion [38] can be a help here. To fix ideas, assume that

$$p(t) = t^m + a_{m-1}t^{m-1} + ... + a_1 t + a_0,$$

and construct the following table

t^0	t^1	t^2	...	t^{m-3}	t^{m-2}	t^{m-1}	t^m
a_0	a_1	a_2	...	a_{m-3}	a_{m-2}	a_{m-1}	1
1	a_{m-1}	a_{m-2}	...	a_3	a_2	a_1	a_0
b_0	b_1	b_2	...	b_{m-3}	b_{m-2}	b_{m-1}	
b_{m-1}	b_{m-2}	b_{m-3}	...	b_2	b_1	b_0	
c_0	c_1	c_2	...	c_{m-3}	c_{m-2}		
c_{m-2}	c_{m-3}	c_{m-4}	...	c_1	c_0		
...	...	...	...	...			
v_0	v_1	v_2					

where

$$b_k = \begin{vmatrix} a_0 & a_{m-k} \\ 1 & a_k \end{vmatrix}$$

for $k = 0, 1, ..., m-1$ (here $a_m = 1$),

$$c_k = \begin{vmatrix} b_0 & b_{m-1-k} \\ b_{m-1} & b_k \end{vmatrix}$$

for $k = 0, 1, ..., m-2$, and so on recursively until we have just three coefficients. Jury's criterion states that the roots of $p(t)$ are inside the unit disk in the complex plane if and only if $p(1) > 0$, $(-1)^m p(-1) > 0$ and $|a_0| < 1$, $|b_0| > |b_{m-1}|$, $|c_0| > |c_{m-2}|$, ..., $|v_0| > |v_2|$.

The Jury's criterion is useful if the coefficients of the polynomial are real numbers, but in general, it is not useful when some parameters appear. This is due to how the coefficients b's, c's and so on are computed. For $m \leq 5$, we can derive from the Jury's criterion the so-called Samuelson's conditions (see

[32, 33]), which somehow simplifies the computations. Another alternative is Rouche's Theorem (see [42] and [3] for an alternative real proof), which states that if

$$|a_{m-1}| + |a_{m-2}| + ... + |a_1| + |a_0| < 1,$$

then, the roots of $p(t)$ are inside the unit open disk of the complex plane. This last condition is, however, sufficient, but it is not necessary. Let us consider the following examples.

Example 2.8. Let us consider the Theocharis oligopoly model with adaptive expectations given by

$$q_{n+1}^{[i]} = \max\left\{0, (1-\lambda)q_n^{[i]} + \lambda\left(\frac{a-c_i}{2b} - \frac{Q_n^{[i]}}{2}\right)\right\},$$

for $i = 1, 2, \ldots, m$, $\lambda \in [0, 1]$, and $a, b > 0$, $a > c_i > 0$. Recall $q_n^{[i]}$ is the production of the firm i at time n, and $Q_n^{[i]} = \sum_{j=1}^m q_n^{[j]} - q_n^{[i]}$ is the residual supply at the same time. Observe that for $\lambda = 0$ the system is trivially constant. On the other hand, $\lambda = 1$ represents "naive expectations", which has already been studied in [16, 25, 57]. The non-zero fixed point , called Cournot point, is given by

$$\overline{q}^{[i]} = \frac{a-(n+1)c_i + nc}{(n+1)b},$$

and the Jacobian matrix at this point is

$$\mathbf{J}_m = \begin{pmatrix} 1-\lambda & -\frac{\lambda}{2} & -\frac{\lambda}{2} & ... & -\frac{\lambda}{2} & -\frac{\lambda}{2} \\ -\frac{\lambda}{2} & 1-\lambda & -\frac{\lambda}{2} & ... & -\frac{\lambda}{2} & -\frac{\lambda}{2} \\ -\frac{\lambda}{2} & -\frac{\lambda}{2} & 1-\lambda & ... & -\frac{\lambda}{2} & -\frac{\lambda}{2} \\ ... & ... & ... & ... & ... & ... \\ -\frac{\lambda}{2} & -\frac{\lambda}{2} & -\frac{\lambda}{2} & ... & 1-\lambda & -\frac{\lambda}{2} \\ -\frac{\lambda}{2} & -\frac{\lambda}{2} & -\frac{\lambda}{2} & ... & -\frac{\lambda}{2} & 1-\lambda \end{pmatrix}.$$

The characteristic polynomial

$$p(t) = |\mathbf{J}_m - t\mathbf{I}_m| = (-1)^m \left(t + \frac{\lambda(m+1)}{2} - 1\right)\left(t + \frac{\lambda}{2} - 1\right)^{m-1},$$

that is the eigenvalues are $1 - \frac{\lambda(m+1)}{2}$ and $1 - \frac{\lambda}{2}$. As $\lambda \in (0, 1]$, the second eigenvalue is always inside the unit disk, so the first one characterizes the stability. Note

$$\left|\frac{\lambda(m+1)}{2} - 1\right| < 1$$

whenever

$$\lambda(m+1) < 4.$$

Example 2.9. We have the delayed Theocharis oligopoly model introduced in [19]

$$q_i(t+1) = (1-\lambda)q_i(t) + \lambda\left(\frac{a-c_i}{2b} - \frac{Q_i(t-k)}{2}\right), \tag{4}$$

where q_i is the output of each firm and $Q_i = (\sum_{i=1}^n q_i) - q_i$ is the residual supply. It is easy to see that the fixed point, Cournot point, $\overline{q}_1, ..., \overline{q}_n$ of this model is the one of the model with $k = 0$. We will assume that $\overline{q}_i > 0$. The Jacobian matrix at the fixed point has its roots inside the unit circle of the complex plane if the polynomials

$$t^{k+1} - (1-\lambda)t^k + \lambda\frac{n-1}{2} \tag{5}$$

and

$$t^{k+1} - (1-\lambda)t^k - \frac{\lambda}{2} \tag{6}$$

have their roots inside that circle. The roots of (6) are inside the circle because

$$1 - \lambda + \frac{\lambda}{2} = 1 - \frac{\lambda}{2} < 1.$$

For the same reason, we see that for $n = 2$ the fixed point is always LAS.

The question of whether LAS implies GAS in a higher dimension is a formidable task which is far from being understood. Some authors have been interested in it in the setting of higher order difference equations; see, for instance, [30, 31]. However, general strategies which can be applied in general are far from being known. It is then an interesting open question which deserves further investigation.

Example 2.10. Now, we consider the Clark's equation

$$x_{n+1} = \lambda x_n + (1-\lambda)f(x_{n-k}),$$

where f is a real map with a negative Schwarzian derivative. It is easy to realize that the fixed points of Clark's equation are the fixed points of f. With an "ad-hoc" argument called dominance, it was proved in [31] that if a fixed point is GAS for f, it is so for Clark's equation. However, it is unclear how this technique can be used for other difference equations.

2.4. *Bifurcations*

As we set before, a fixed point $\mathbf{x}_0$ is said to be non-hyperbolic if the Jacobian matrix $\mathbf{Jf}(\mathbf{x}_0)$ has an eigenvalue with modulus equal to one. Usually, the map $\mathbf{f}$ depends on one or several parameters. The codimension refers to the number of parameters which are necessary to observe the bifurcation phenomena. For instance, let us fix that $\mathbf{f}(\mathbf{x}, \alpha)$, where $\alpha \in (-a, a)$, $a > 0$, is a parameter. Assume that $\mathbf{x}_0(\alpha)$ is a fixed point such that $\mathbf{x}_0(0)$ is non-hyperbolic. In this case, the local dynamics may be different with negative values of α to that obtained with positive values, being $\alpha = 0$ a bifurcation value.

When the phase space X is an interval of the real line and $f : X \to X$ is smooth enough, there are just two ways of losing the stability, namely either $f'(x_0(0), 0) = 1$ or $f'(x_0(0), 0) = -1$. In the first case, we have the so-called fold (also saddle-node) bifurcation, in which the fixed point loses its stability, and two new fixed points appear, one of them LAS and the other unstable. The following result (see, e.g., [40]) gives us sufficient conditions for this bifurcation.

Theorem 2.11. *Let $f(x, \alpha)$ be smooth enough with respect to x and α, and assume that $f'(x_0(0), 0) = \frac{\partial f}{\partial x}(x_0(0), 0) = 1$ and the following conditions are fulfilled:*

(a) $\frac{\partial f}{\partial \alpha}(x_0(0), 0) \neq 0$.

(b) $\frac{\partial^2 f}{\partial x^2}(x_0(0), 0) \neq 0.$

Then, the fixed point $x_0(0)$ loses its stability through a fold bifurcation.

Example 2.12. Now, we consider the γ-Ricker model given by the map $f_{A,\gamma}(x) = Ax^\gamma e^{-x}$. Recall that a non-zero fixed point satisfies that

$$Ax_0^{\gamma-1} e^{-x_0} = 1,$$

and when the derivative is equal to one, then $x_0 = \gamma - 1$. Then we compute

$$\frac{\partial f_{A,\gamma}}{\partial A}(\gamma - 1) = (\gamma - 1)^\gamma e^{1-\gamma} \neq 0,$$

and

$$\frac{\partial^2 f_{A,\gamma}}{\partial x^2}(\gamma - 1) = -A(\gamma - 1)^{\gamma-1} e^{1-\gamma} \neq 0.$$

So, for any fixed value of γ, we have that for

$$A = \left(\frac{e}{\gamma - 1}\right)^{\gamma-1}$$

the fixed point $\gamma - 1$ destabilizes following a fold bifurcation. Note here that $\gamma - 1$ is semistable since $f''(\gamma - 1) = -Ae^{\gamma-1}(\gamma - 1)^{\gamma-1} < 0$.

Example 2.13. In the logistic model $f_a(x) = ax(1 - x)$, the fixed point 0 does not destabilize via a fold bifurcation at $a = 1$. It follows a transcritical bifurcation in which two fixed points change their stability, one stable and the other unstable. Here 0 is stable and destabilizes while $\frac{a-1}{a}$ does the opposite (see [62]). Note that this second fixed point is negative for $a < 1$, so we do not note it when one considers only positive values of x. The sufficient conditions for transcritical bifurcation consist of replacing (a) of Theorem 2.11 by

$$\frac{\partial^2 f}{\partial \alpha \partial x}(x_0(0), 0) \neq 0.$$

Note that for the logistic case, this condition is

$$\frac{\partial^2 f_a}{\partial a \partial x}(x_0(0), 0) = 1.$$

Yet, another possible codimension one bifurcation appears associated with the derivative equal to one. It is called Pitchfork bifurcation, and here a stable fixed point loses its stability, and two new stable fixed points appear (see [62]). The sufficient conditions for Pitchfork bifurcation consist of replacing (a) and (b) of Theorem 2.11, which are not satisfied, by

$$\frac{\partial^2 f}{\partial \alpha \partial x}(x_0(0), 0) \neq 0,$$

and

$$\frac{\partial^3 f}{\partial x^3}(x_0(0), 0) \neq 0.$$

Example 2.14. Consider the map $\varphi_a(x) = ax - x^3$, $a > 0$, defined in the whole real line. This map has 0, a fixed point for all a, and two additional fixed points $\pm\sqrt{a-1}$ for $a > 1$. At $a = 1$ we have that $\varphi_1'(0) = 1$ while $0 < \varphi_a'(0) < 1$ for $a \in (0, 1)$. The fixed points $\pm\sqrt{a-1}$ become stable for $a \in (1, 2)$.Here, we have a Pitchfork bifurcation since $\frac{\partial^2 \varphi_a}{\partial a \partial x}(0) = 1$ and $\frac{\partial^3 \varphi_a}{\partial x^3}(0) = -6$. Notice that $\frac{\partial^2 \varphi_a}{\partial x^2}(0) = 0$.

Remark 2.15. *Regarding the Pitchfork bifurcation, we must mention that when* $\frac{\partial^2 f}{\partial x^2}(x_0(0), 0) = 0$*, some authors consider this bifurcation of codimension two. For instance, in [40], it is considered a cusp bifurcation which depends on two parameters, and the normal form is of type* $x + \alpha_1 + \alpha_2 x \pm x^3$*. We include it here in the codimension one because the family we consider depends on one parameter. However, the phenomenon is the same as in the above normal form when* $\alpha_1 = 0$*.*

Now we assume that $f'(x_0(0)) = -1$. In this case, the destabilization is produced via a flip (also period-doubling) bifurcation in which the LAS fixed point loses its stability and a LAS periodic orbit of period two appears. As in the fold case, we have the following result.

Theorem 2.16. *Let* $f(x, \alpha)$ *be smooth enough and assume that* $f'(x_0(0), 0) = -1$ *and the following conditions are fulfilled:*

(a) $\frac{\partial^2 f}{\partial \alpha \partial x}(x_0(0), 0) \neq 0$.

(b) $\frac{1}{2}\left(\frac{\partial^2 f}{\partial x^2}(x_0(0), 0)\right)^2 + \frac{1}{3}\frac{\partial^3 f}{\partial x^3}(x_0(0), 0) \neq 0$.

Then, the fixed point $x_0(0)$ *loses its stability through a flip bifurcation.*

Example 2.17. Again, we consider the logistic model $f_a(x) = ax(1-x)$. The fixed point $\frac{a-1}{a}$ destabilizes via a flip bifurcation at $a = 3$ since

$$\frac{\partial^2 f_a}{\partial a \partial x}\left(\frac{2}{3}\right) = -\frac{1}{3}$$

and

$$\frac{1}{2}\left(\frac{\partial^2 f_a}{\partial x^2}\left(\frac{2}{3}\right)\right)^2 + \frac{1}{3}\frac{\partial^3 f_a}{\partial x^3}\left(\frac{2}{3}\right) = 18.$$

The well-known bifurcation of the logistic map is shown in Figure 2. It shows the famous period-doubling cascade to chaos in which each periodic orbit of period 2^m bifurcates to a new LAS periodic point of period 2^{m+1}, $m \geq 0$. When the parameter $a > 3.5699...$, the dynamics become chaotic. We will characterize chaos in the next section.

With one parameter and dimension one, fold and flip bifurcation is what we have. In dimension two, a new codimension one bifurcation appears, namely Neimark-Sacker bifurcation. Now, the fixed point loses its stability, and a stable invariant curve appears. This happens because the eigenvalues at the bifurcation parameter are complex numbers of modulus one.

To check the existence of this bifurcation, we need to introduce the following technical notation (see [40, 41]). Let $\mathbf{f}(x, y, \alpha)$ be smooth enough such that the eigenvalues of the Jacobian matrix at the fixed point $(x_0(\alpha), y_0(\alpha))$ are

$$\mu_{\pm}(\alpha) = r(\alpha)e^{\pm i\theta(\alpha)},$$

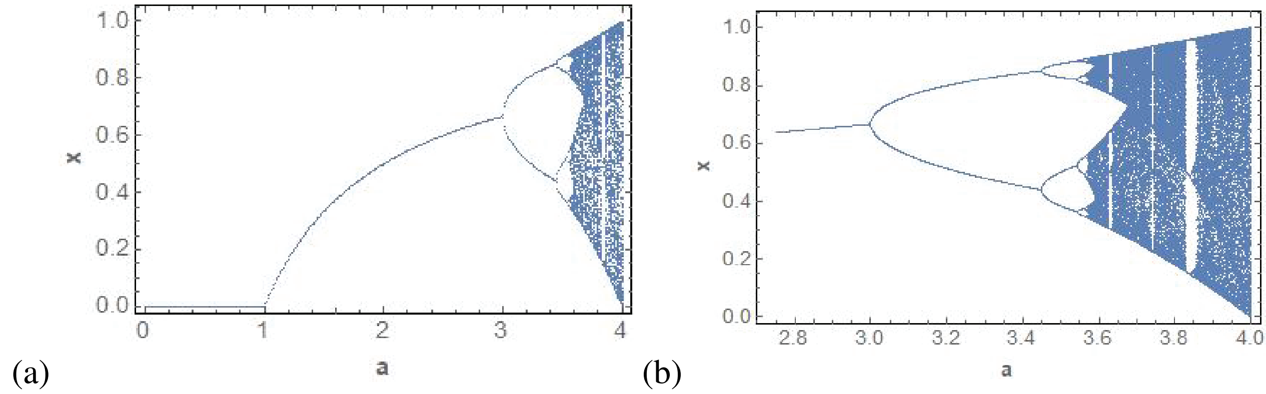

Figure 2. *(a) Bifurcation diagram of the logistic map for $a \in (0, 4]$ with step size 10^{-2}. We see the existence of a fold bifurcation at $a = 1$ and a flip bifurcation at $a = 3$. Next, we check the cascade of period-doubling bifurcation of periodic orbit until arriving in the chaotic region. (b) shows an enlargement of the bifurcation diagram for $a \in [2.75, 4]$ with step size 10^{-3}.*

with $r(0) = 1$. Consider $\langle\ ,\ \rangle$ the scalar product on $\mathbb{C}^2$ and denote $\mathbf{A} = \mathbf{Jf}(x_0(0), y_0(0), 0)$. Consider $\mathbf{p}, \mathbf{q} \in \mathbb{C}^2$ with $\langle \mathbf{p}, \mathbf{q} \rangle = 1$ and such that $\mathbf{A} \cdot \mathbf{q} = e^{i\theta(0)}\mathbf{q}$ and $\mathbf{A}^T \cdot \mathbf{p} = e^{-i\theta(0)}\mathbf{p}$ (here $\mathbf{A}^T$ is the transpose of $\mathbf{A}$). For $i = 1, 2$ and $\mathbf{x} = (x_1, x_2), \mathbf{y} = (y_1, y_2), \mathbf{z} = (z_1, z_2) \in \mathbb{R}^2$, let

$$B_i(\mathbf{x}, \mathbf{y}) = \frac{\partial^2 f_i}{\partial x^2}(x_0(0), y_0(0), 0)x_1y_1 + \frac{\partial^2 f_i}{\partial x \partial y}(x_0(0), y_0(0), 0)(x_1y_2 + x_2y_1) + \frac{\partial^2 f_i}{\partial y^2}(x_0(0), y_0(0), 0)x_2y_2$$

and

$$\begin{aligned} C_i(\mathbf{x}, \mathbf{y}, \mathbf{z}) &= \frac{\partial^3 f_i}{\partial x^3}(x_0(0), y_0(0), 0)x_1y_1z_1 + \frac{\partial^3 f_i}{\partial x^2 \partial y}(x_0(0), y_0(0), 0)(x_1y_1z_2 + x_1y_2z_1 + x_2y_1z_1) \\ &\quad + \frac{\partial^3 f_i}{\partial x \partial y^2}(x_0(0), y_0(0), 0)(x_1y_2z_2 + x_2y_1z_2 + x_2y_2z_1) + \frac{\partial^3 f_i}{\partial y^3}(x_0(0), y_0(0), 0)x_2y_2z_2, \end{aligned}$$

where f_i, $i = 1, 2$, are the coordinate functions of $\mathbf{f}$. Denoting by $\mathbf{I}_2$ the identity matrix, $\mathbf{B} = (B_1, B_2)$ and $\mathbf{C} = (C_1, C_2)$, we compute

$$d = e^{-i\theta} \left\langle \mathbf{p}, \mathbf{C}(\mathbf{q}, \mathbf{q}, \overline{\mathbf{q}}) + 2\mathbf{B}(\mathbf{q}, (\mathbf{I}_2 - \mathbf{A})^{-1}\mathbf{B}(\mathbf{q}, \overline{\mathbf{q}})) + \mathbf{B}(\overline{\mathbf{q}}, (e^{2\theta i}\mathbf{I}_2 - \mathbf{A})^{-1}\mathbf{B}(\mathbf{q}, \mathbf{q})) \right\rangle.$$

The sufficient conditions are stated as follows.

Theorem 2.18. *Let $\mathbf{f}(x, y, \alpha)$ be smooth enough such that the eigenvalues of the Jacobian matrix at the fixed point $(x_0(\alpha), y_0(\alpha))$ are*

$$\mu_\pm(\alpha) = r(\alpha)e^{\pm i\theta(\alpha)},$$

with $r(0) = 1$. If the following conditions are fulfilled

(a) $e^{k\theta(0)} \neq 1$ *for* $k = 1, 2, 3, 4$.

(b) $r'(0) \neq 0$.

(c) $c = \mathrm{Re}(d) \neq 0$.

Then the fixed point destabilizes via a Neimark-Sacker bifurcation.

Example 2.19. We consider the delayed Ricker equation

$$x_{n+1} = Ax_n e^{-x_{n-1}}, \quad A \geq 1,$$

and its associate order one system

$$\begin{cases} y_{n+1} = x_n, \\ x_{n+1} = Ax_n e^{-y_n}. \end{cases}$$

The non-zero fixed point is $x_0 = \log A$. Given $f_A(y, x) = Axe^{-y}$, the characteristic polynomial at (x_0, x_0) is

$$p(t) = t^2 - \frac{\partial f_A}{\partial x}(x_0, x_0)t - \frac{\partial f_A}{\partial y}(x_0, x_0) = t^2 - t + \log A,$$

so when $1 - 4\log A < 0$ we have complex eigenvalues. Note that their modulus is

$$r(A) = \sqrt{\log A}.$$

So, the condition for them having modulus one is $A = e$. We left the reader to check the conditions of Theorem 2.18. Note that we have to apply it to the map $\mathbf{f}_A(y, x) = (x, f_A(y, x))$.In Figure 3, we show the existence of the invariant curve.

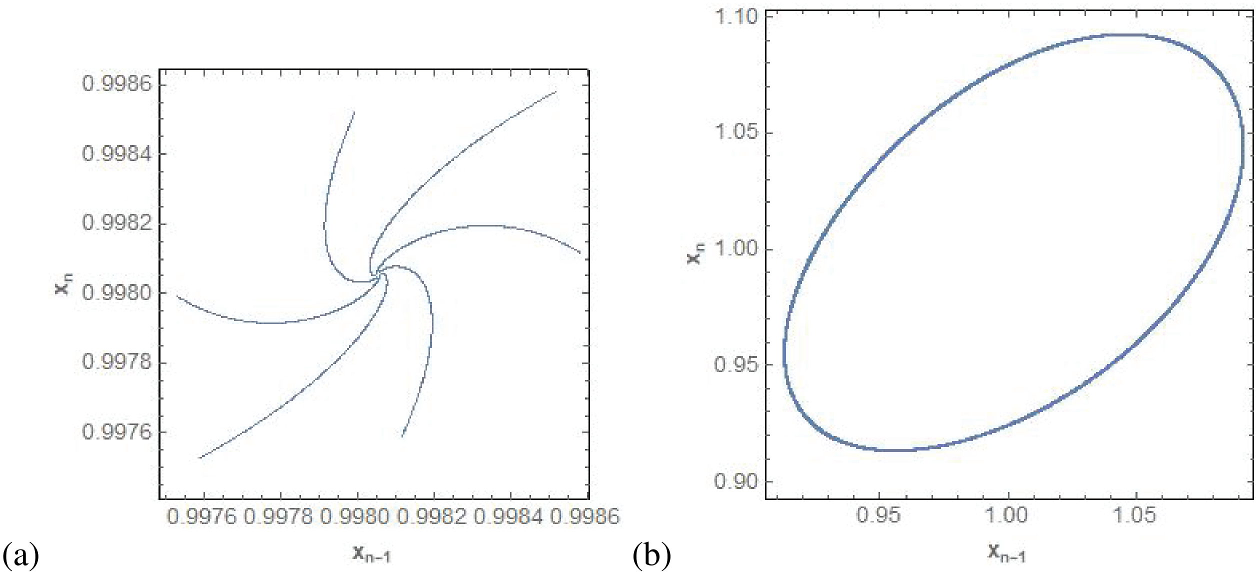

Figure 3. *We show the breeding of an invariant curve when $a = e$ follows the Neimark-Sacker bifurcation. We depict the stable fixed point for $a = 2.713$ and the invariant curve for $a = 2.721$.*

If we increase the dimension and codimension, we can have more types of bifurcations exhibiting richer dynamics. For this review, the above contents are enough, but we refer the reader to e.g. [40] to read more about bifurcations on discrete-time models. In the next section, we will go beyond periodic orbits and analyze the notion of chaos in discrete dynamics.

3. Beyond periodic motions: chaos

The bifurcation diagram of Figure 2 shows that there are ω-limit sets which are not periodic. In addition, although many ω-limit sets can coexist, even infinitely many, some of them are especially relevant.

For instance, let us consider the map $f(x) = 3.83x(1-x)$. Let us fix an initial condition randomly and compute an orbit of length 1000. One can see that the orbit seems to converge to the periodic orbit given by the points $0.50467...$, $0.95742...$ and $0.15615...$. We consistently arrive at the same result when repeating the experiment. According to Sharkovsky's Theorem, this system has infinitely many periodic orbits, although all of them seem to be hidden except for that periodic orbit.

Sharkovsky's Theorem (see [52], [2] or [28] for a simple proof) tells us that the above system has infinitely many different periodic orbits. This result reads as follows. We order the natural numbers as follows:

$$3 >_s 5 >_s 7 >_s ... >_s 2 \cdot 3 >_s 2 \cdot 5 >_s 2 \cdot 7 >_s ...$$
$$2^n \cdot 3 >_s 2^n \cdot 5 >_s 2^n \cdot 7 >_s ... >_s 2^{n+1} >_s 2^n >_s ... >_s 2 >_s 1.$$

For $n \in \mathbb{N} \cup \{2^\infty\}$ define $\mathcal{S}(n) = \{m \in \mathbb{N} : n >_s m\} \cup \{n\}$ and $\mathcal{S}(2^\infty) = \{2^n : n \in \mathbb{N} \cup \{0\}\}$. Then, we can state the following result.

Theorem 3.1. *Let $f : X \subset \mathbb{R} \to X$ be a continuous map defined on an interval X. If f has a periodic orbit of period n, then it has periodic points of period $m \in \mathcal{S}(n)$. Moreover, for any $n \in \mathbb{N} \cup \{2^\infty\}$ there is $f_n \in C(X)$ such that its set of periods is $\mathcal{S}(n)$.*

As the above periodic orbit has period three, Theorem 3.1 guarantees that we have periodic orbits of all the possible periods. Not all the possible ω-limit sets are detected via a numerical simulation. The following definition explains the situation.

A set $\Omega \subset X$ is called a forward invariant under f if $f(\Omega) \subseteq \Omega$. It is strongly forward invariant if $f(\Omega) = \Omega$. The basin of attraction of a forward invariant set Ω, $B(\Omega)$ is given by

$$B(\Omega) = \{x : \omega(x, f) \subseteq \Omega\}.$$

Following Milnor [46], a forward invariant set Ω is called a (minimal) metric attractor if $B(\Omega)$ has positive Lebesgue measure and if Ω' is a forward invariant compact set strictly contained in Ω then $B(\Omega')$ has Lebesgue measure equal to zero. $B(\Omega)$ is called the basin of the attractor. For some smooth enough interval maps, the number of Milnor attractors can be characterized as follows.

We are interested in piecewise monotone maps. Let $X = [a, b] \subset \mathbb{R}$ and consider $f : X \to X$ a continuous interval map such that there are $a = c_0 < c_1 < ... < c_i = b$ such that for each $1 \leq j \leq i-1$ it holds that c_j is a local extrema of f, with $f|_{[c_j, c_{j+1}]}$ strictly monotone for $j = 0, 1, ..., i-1$. The points c_j, $j = 1, ..., i-1$, are called turning points of f. Note that if f is differentiable, then $f'(c_j) = 0$ for $j = 1, ..., i-1$. In addition (see [60]), we will assume that the map f is smooth enough, in our case C^2 or C^3, and the turning points are non-flat, that is, for x close to c_j, $j = 1, 2, ..., i-1$,

$$f(x) = \pm|\phi(x)|^{\beta_i} + f(c_j),$$

where ϕ is C^3, $\phi(c_j) = 0$ and $\beta_i > 0$. An interval $J \subset X$ is called wandering if the intervals $\{J, f(J), \ldots, f^n(J), \ldots\}$ are pairwise disjoint and if J is not contained in the basin of an attracting periodic orbit of f. Then, we have the following result (see [60]).

Theorem 3.2. *Let $f : X \to X$ be a $\mathcal{C}^2$ piecewise monotone map with non flat turning points. Then f has no wandering intervals.*

In addition, if the map f is C^3 and piecewise monotone there are three possibilities for its metric attractors:

A1) A periodic orbit (recall that x is periodic if $f^n(x) = x$ for some $n \in \mathbb{N}$).

A2) A union of periodic intervals $J_1, ..., J_k$, such that $f^k(J_i) = J_i$ and $f^k(J_i) = J_j$, $1 \leq i < j \leq k$, and such that f^k is topologically mixing. Topologically mixing property implies the existence of dense orbits on each periodic interval (under the iteration of f^k).

A3) A minimal (every orbit is dense) Cantor set $\omega(c, f)$ such that $c \in \omega(c, f)$ is a turning point.

Moreover, if f has an attractor of type (A2) and (A3), then they must contain the orbit of a turning point, and therefore, the turning points bound its number. Moreover, for each critical point c that is not in the basin of a periodic attractor, there exists a neighborhood U such that whenever $f^n(x) \in U$ for some $x \in X$ and some $n \in \mathbb{N}$, then the Schwarzian derivative of f^{n+1} at x is negative, that is, $\mathcal{S}(f^{n+1})(x) < 0$.

The above result cannot apply to periodic attractors. If we add the condition of negative Schwarzian derivative, then we have the following result that can be found in [53].

Theorem 3.3. *Let $f : I \to I$ be a $\mathcal{C}^3$ interval map with $\mathcal{S}(f)(x) < 0$ for each $x \in [0, 1]$ such that $f'(x) \neq 0$. Then, each attracting periodic orbit attracts at least one critical point or boundary point.*

Let us illustrate the above results with several examples.

Example 3.4. We consider the γ-Ricker map given by $f_{A,\gamma}(x) = Ax^\gamma e^{-x}$, $x \geq 0$. The Schwarzian derivative of $f_{A,\gamma}$ holds that

$$\mathcal{S}(f_{A,\gamma})(x) = -\frac{(x-\gamma)^4 + 4\gamma x - \gamma^2}{2(\gamma - x)^2 x^2} < 0.$$

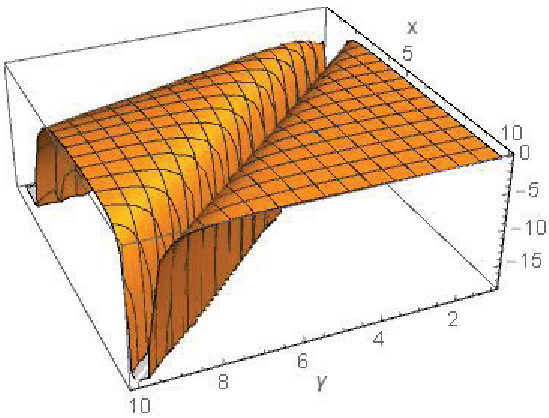

Figure 4. *We depict the graph of the Schwarzian derivative of the γ-Ricker map.*

Figure 4 shows the graph of the Schwarzian derivative of $f_{A,\gamma}$. As the fixed point 0 is always LAS, we have that $f_{A,\gamma}$ can have at most two Milnor attractors. When

$$A < A_0(\gamma) := \left(\frac{e}{\gamma - 1}\right)^{\gamma - 1}$$

the fixed point 0 is not only LAS but also GAS. For $A \geq A_0(\gamma)$, a new Milnor attractor appears. All of them are of the form (A1)-(A3) stated before. Bifurcation diagrams for some fixed values of γ can be seen in Figure 5.

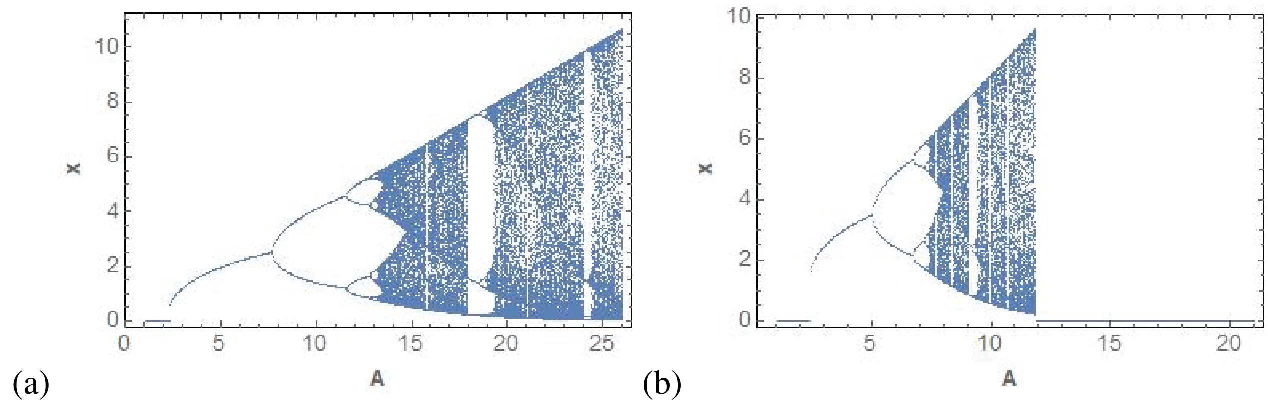

Figure 5. *Bifurcation diagram of the γ-Ricker map for $\gamma = 1.5$(a) and $\gamma = 2.5$(b). We fix $a \in (0, 4]$ with step size 0.05. Note that in (b), we have extinction for A close to one and after the parameter reaches the chaotic region. We will call the last phenomenon almost sure extinction, and it will be related to the topological entropy.*

3.1. *Several definitions of chaos*

There are many definitions of chaos, but we will focus our interest on the following well-known ones. We consider $\mathbf{f} : X \to X$, $X \subseteq \mathbb{R}^d$ and denote by $|| \; ||$ the Euclidean norm. The map $\mathbf{f}$ is chaotic in the sense of Li and Yorke (LY-chaotic) [43] if there is an uncountable set S (called a scrambled set of $\mathbf{f}$) such that for any $\mathbf{x}, \mathbf{y} \in S$, $\mathbf{x} \neq \mathbf{y}$, we have that

$$0 = \liminf_{n\to\infty} ||\mathbf{f}^n(\mathbf{x}) - \mathbf{f}^n(\mathbf{y})|| < \limsup_{n\to\infty} ||\mathbf{f}^n(\mathbf{x}) - \mathbf{f}^n(\mathbf{y})||.$$

Li and Yorke's definition of chaos became famous because it is known that the existence of a periodic orbit of period three implies the existence of chaos. This result links periodic orbits and unpredictable dynamical behavior for continuous interval maps. Note that the definition implies the comparison between two orbits or limit points of orbits. Another well-known chaos definition, inspired by the notion of sensitivity with respect to the initial conditions [36], was given by Devaney [27] as follows. Assume that X is compact. The map $\mathbf{f}$ is said to be chaotic in the sense of Devaney (D–chaotic) if it fulfils the following properties:

- The map f it is transitive, which in absence of isolated points means that there is $\mathbf{x} \in X$ such that $\omega(\mathbf{x}, \mathbf{f}) = X$.
- The set of periodic points $\mathrm{P}(\mathbf{f})$ is dense on X.
- It has sensitive dependence on initial conditions, that is, there is $\varepsilon > 0$ such that for any $\mathbf{x} \in X$ there is an arbitrarily close $\mathbf{y} \in X$ and $n \in \mathbb{N}$ such that $||\mathbf{f}^n(\mathbf{x}) - \mathbf{f}^n(\mathbf{y})|| > \varepsilon$[1].

Both Li-Yorke chaos and sensitivity to initial conditions are part of the dynamical systems folklore. There are a lot of different stages between periodic orbits and chaotic behavior, so it is interesting to explain simple dynamics. Sometimes, chaotic behavior can also be taken as the opposite of simple (or ordered) behavior. We say that $\mathbf{f}$ is strongly simple (ST-simple) if any ω-limit set is a periodic orbit of

1. It is proved in [8] that the first two conditions in Devaney's definition imply the third one. The definitions are presented in the original form because of the dynamical meaning of sensitive dependence on initial conditions.

$\mathbf{f}$. We say that an orbit $\mathrm{Orb}(\mathbf{x}, \mathbf{f})$, $\mathbf{x} \in X$, is approximated by periodic orbits if for any $\varepsilon > 0$ there is $\mathbf{y} \in \mathrm{P}(\mathbf{f})$ and $n_0 \in \mathbb{N}$ such that$||\mathbf{f}^n(\mathbf{x}) - \mathbf{f}^n(\mathbf{y})|| < \varepsilon$ for all $n \geq n_0$. The map $\mathbf{f}$ is LY-simple [55] if any orbit is approximated by periodic orbits. Finally, $\mathbf{f}$ is Lyapunov stable (L-simple) [34] if it has equicontinuous powers.

Example 3.5. We consider the γ-Ricker model with $\gamma = 1.5$. We fix the values of $A \in \{11.5, 22\}$. In Figure 6, we depict the time series of the initial condition $x_0 = \gamma$. We observe both chaotic and non-chaotic behavior. Below, we will see how to find the values of A to exhibit these behaviors.

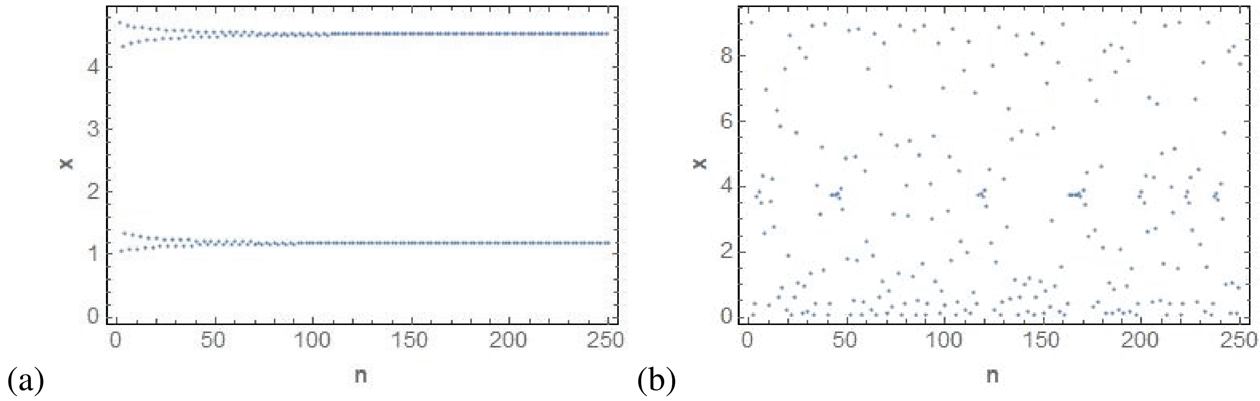

Figure 6. *Fix $\gamma = 1.5$ and depict the time series is size 250 with initial condition 1.5 for $A = 11.5$(a) and $A = 22$(b). While (a) shows the convergence to a periodic point of period two, the time series shown in (b) seems unpredictable.*

The above definitions are quite challenging to verify, especially when working with models that may depend on several parameters. Thus, we need some practical methods to measure the dynamic complexity of the system. One of them is given by topological entropy, which was introduced in the setting of continuous maps on compact topological spaces by Adler, Konheim and McAndrew [1] and Bowen [15]. For continuous real maps, the definition reads as follows. Given $\varepsilon > 0$, we say that a set $E \subset X$ is $(n, \varepsilon, \mathbf{f})$–separated if for any $\mathbf{x}, \mathbf{y} \in E$, $\mathbf{x} \neq \mathbf{y}$, there exists $k \in \{0, 1, ..., n-1\}$ such that $||\mathbf{f}^k(\mathbf{x}) - \mathbf{f}^k(\mathbf{y})|| > \varepsilon$. Denote by $s\,(n, \varepsilon, \mathbf{f})$ the biggest cardinality of any maximal $(n, \varepsilon, \mathbf{f})$–separated set in X. Then, the topological entropy of $\mathbf{f}$ is

$$h\,(\mathbf{f}) = \lim_{\varepsilon \to 0} \limsup_{n \to \infty} \frac{1}{n} \log s\,(n, \varepsilon, \mathbf{f})\,.$$

An equivalent definition using spanning sets is given below. We say that a set $F \subset X$ $(n, \varepsilon, \mathbf{f})$-spans X if for any $\mathbf{x} \in X$ there exists $\mathbf{y} \in F$ such that $||\mathbf{f}^i(\mathbf{x}) - \mathbf{f}^i(\mathbf{y})|| < \varepsilon$ for any $i \in \{0, 1, ..., n-1\}$. Denote by $r\,(n, \varepsilon, \mathbf{f})$ the smallest cardinality of any minimal $(n, \varepsilon, \mathbf{f})$–spanning set in X. Then, topological entropy can be computed as

$$h\,(\mathbf{f}) = \lim_{\varepsilon \to 0} \limsup_{n \to \infty} \frac{1}{n} \log r\,(n, \varepsilon, \mathbf{f})\,.$$

In general, the above chaos definitions are not equivalent, and their relations with topological entropy are not homogeneous, but for continuous interval maps, the connections among them are well-known and related to Sharkovsky's theorem. For real a real map f, we say that it is S-chaotic it it has a periodic orbit which is not a period of two. On the other hand, for one-dimensional dynamics, the topological entropy is a useful tool to check the dynamical complexity of a map because it is strongly connected with the notion of horseshoe (see [2, page 205]). We say that a real map $f : X \to X$ has a k-horseshoe, $k \in \mathbb{N}$, $k \geq 2$, if there are k disjoint subintervals J_i, $i = 1, ..., k$, such that $J_1 \cup ... \cup J_k \subseteq f(J_i)$, $i = 1, ..., k^2$.

The following result shows some equivalences among the above definitions of chaos and order (see [52], [55] and [12]).

Theorem 3.6. *Let $f : X \to X$ be a continuous map. Then*

(a) The map f has positive topological entropy if and only if the map f is S-chaotic.

(b) If f is D-chaotic, then $h(f) > 0$.

(c) If f is either ST-simple or L-simple, then $h(f) = 0$.

(d) If $h(f) > 0$, then f is LY-chaotic, but the converse is false in general. If f is LY-simple, then $h(f) = 0$. The union of LY-chaotic and LY-simple continuous maps is the set of continuous interval maps.

If we consider more regularity conditions on the map f, for instance, C^3 without flat turning points for multimodal maps, we have that there are no LY-chaotic maps with zero topological entropy and hence, topological entropy is a tool to decide whether a map is LY-chaotic [4].

3.2. *Chaos measurement*

Next, we deal with the practical computation of the topological entropy to characterize the complicated dynamical behavior. However, Bowen's topological entropy definitions are unsuitable for working with families of interval maps depending on parameters. Then, in practice, some algorithms are needed to compute. For unimodal maps (see [13]), it is possible to make the computations using the turning point. Let f be a unimodal map with maximum (turning point) at c. Let $k(f) = (k_1, k_2, k_3, ...)$ be its kneading sequence given by the rule

$$k_i = \begin{cases} R & \text{if } f^i(c) > c, \\ C & \text{if } f^i(c) = c, \\ L & \text{if } f^i(c) < c. \end{cases}$$

We fix that $L < C < R$. For two different unimodal maps f_1 and f_2, we fix their kneading sequences $k(f_1) = (k_n^1)$ and $k(f_2) = (k_n^2)$. We say that $k(f_1) \leq k(f_2)$ provided there is $m \in \mathbb{N}$ such that $k_i^1 = k_i^2$ for $i < m$ and either an even number of $k_i^1{}'s$ are equal to R and $k_m^1 < k_m^2$ or an odd number of $k_i^1{}'s$ are equal to R and $k_m^2 < k_m^1$. Then it is proved in [13] that if $k(f_1) \leq k(f_2)$, then $h(f_1) \leq h(f_2)$. In addition, if $k_m(f)$ denotes the first m symbols of $k(f)$, then if $k_m(f_1) < k_m(f_2)$, then $h(f_1) \leq h(f_2)$.

The algorithm for computing the topological entropy is based in the fact that the tent family

$$g_s(x) = \begin{cases} sx & if \quad x \in [0, 1/2], \\ -sx + s & if \quad x \in [1/2, 1], \end{cases}$$

2. Since Smale's work (see [56]), horseshoes have been in the core of chaotic dynamics, describing what we could call random deterministic systems.

with $s \in [1,2]$, holds that $h(g_s) = \log s$. The algorithm's idea is to bound the topological entropy of an unimodal map between the topological entropies of two tent maps. The algorithm is divided into four steps:

Step 1. Fix $\varepsilon > 0$ (fixed accuracy) and an integer m. Fix $a = 1$, $b = 2$ and $s = \frac{a+b}{2}$.

Step 2. Compute $k_m(f)$ for a fixed unimodal map f. Compute $k_m(g_s)$.

Step 3. If $k_m(g_s) < k_m(f)$, then set $a = s$ and $b = b$. Otherwise set $a = a$ and $b = s$.

Step 4. Repeat this process until $\log(\frac{a+b}{2}) < \varepsilon$.

The algorithm is easily programmed. We usually use Mathematica, which has the advantage of computing the kneading invariants of tent maps without round-off errors, improving the method's accuracy in practice. If the program runs correctly, one can be confident that the topological entropy will be $h(f) = \log(\frac{a+b}{2})$ with an accuracy smaller than ε. Note that this algorithm is slightly different from that of [13] and can be found in its present form in [23].

The ideas of the above algorithm can be extended into more general settings. For maps with two extrema (bimodal maps), an algorithm can be found in [14]. It was noticed in [21] that the algorithm depends on the number of turning points with different forward images, so the algorithm from [14] can be adapted to multimodal maps. If we increase the number of turning points with different forward images to three, an algorithm can be found in [22]. The reader is referred to [23] for a review on this topic.

Example 3.7. We consider the γ-Ricker map $f_{A,\gamma}(x) = Ax^\gamma e^{-x}$. This map is unimodal; it has a non-zero turning point at $x_M = \gamma$. Although $f_{A,\gamma}$ is not defined on a compact subinterval, note that $f_{A,\gamma}([0,\infty)) = [0, f_{A,\gamma}(\gamma)]$ and $f_{A,\gamma}([0, f_{A,\gamma}(\gamma)]) \subseteq [0, f_{A,\gamma}(\gamma)]$. So, we can apply the algorithm to compute the topological entropy. Fix an accuracy of 10^{-4}. Figure 7 shows the result of our computations for $\gamma \in [1,3]$ and $A \in [1,20]$.

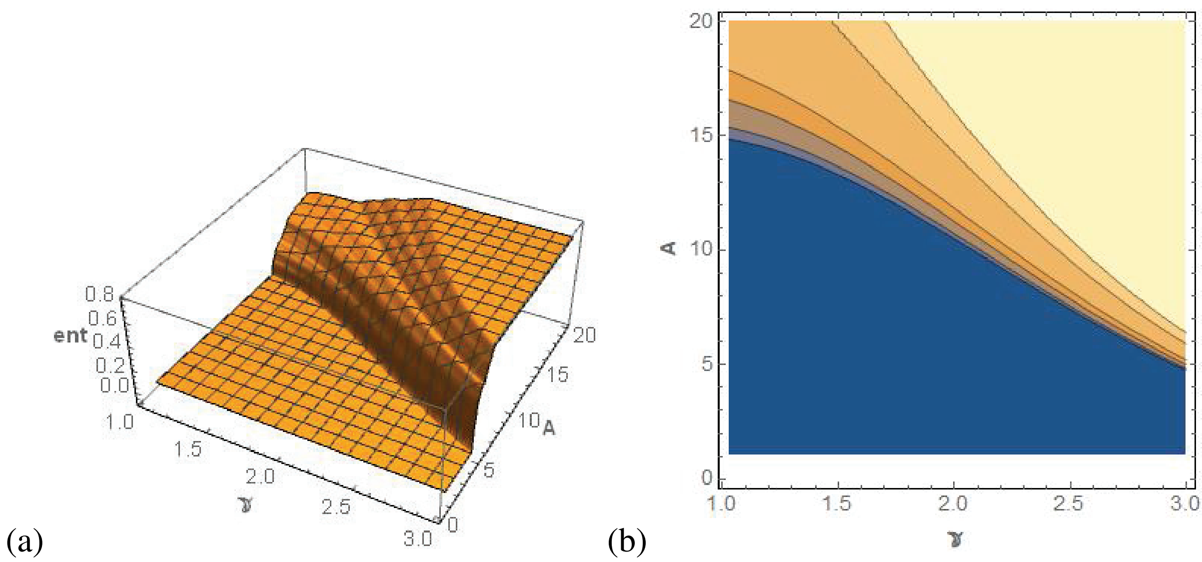

Figure 7. *(a) Topological entropy of γ-Ricker model. (b) Level curves of the topological entropy of the γ-Ricker model.*

We also compute the topological entropy for $\gamma = 2.5$ of Example 3.4. We can see how the phenomenon of almost sure extinction happens when the topological entropy attains its maximum value $\log 2$. The computations are shown in Figure 8.

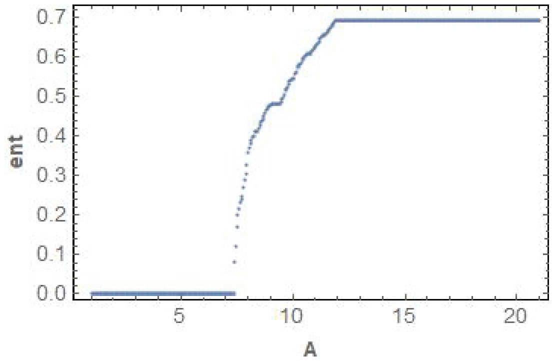

Figure 8. *Topological entropy of γ-Ricker model for $\gamma = 2.5$ and $A \in [1, 21]$. It can be checked that the highest value of topological entropy is $\log 2$, that is attained at the zone of almost sure extinction. The dynamics is chaotic but there is a unique attractor 0, so we only observe the extinction of the population.*

Recall that chaos is a topological notion, and then it cannot be detected with a numerical simulation in some cases. To characterize this phenomenon in one dimensional dynamics we have the so-called Lyapunov exponents (see [47]). For $x \in X$ we define the Lyapunov exponent at x as

$$\operatorname{lex}(x) = \lim_{n\to\infty} \frac{1}{n} \log |(f^n)'(f(x))| = \lim_{n\to\infty} \frac{1}{n} \sum_{j=1}^{n} \log |f'(f^j(x))|,$$

provided the limit exists. Otherwise, we can take limit superior in the definition. If $\{c_1, ..., c_{i-1}\}$ are the turning points of f, then $\operatorname{lex}(c_j)$ will be negative when the orbit of the turning point converges to a periodic orbit. In other words, chaos can be detected in a numerical simulation if the Lyapunov exponent is positive.

Example 3.8. We consider the γ-Ricker map $f_{A,\gamma}(x) = Ax^\gamma e^{-x}$ and estimate the Lyapunov exponents $\operatorname{lex}(\gamma)$ for the parameter values of Example 3.7. The result is shown in Figure 9.

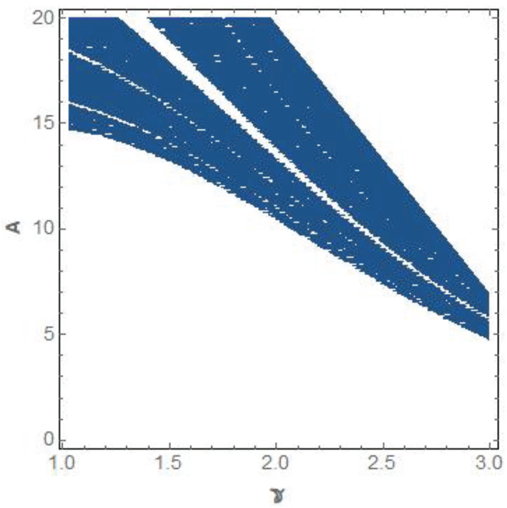

Figure 9. *For $\gamma \in [1, 3]$ and $A \in [1, 21]$, in blue we depict the region where the Lyapunov exponents are positive and hence, chaos is physically observable.*

3.3. *Higher dimensions*

When we deal with a model of a dimension greater than one, the techniques available for characterizing the complicated behavior are not developed in the form they are for one-dimensional models. In particular, there are not algorithms for computing the topological entropy. Although Lyapunov exponents can be estimated here, we really do not know what are the points that play the role of turning points (in the case they exist). So, we have an additional problem; we do not know either the number of attractors or their topological and metric structure. Here, we will show a rough way to grasp some information from the model.

First, we take some ideas from Ergodic Theory (see [61]). Given a continuous map $\mathbf{f} : X \to X$, we consider the σ-algebra of Borel sets of X and let $M(X)$ be the set of probability measures on it. A measure $\mu \in M(X)$ is invariant for $\mathbf{f}$ is $\mu(\mathbf{f}^{-1}(A)) = \mu(A)$ for all Borel set A. If X is compact, then the set of invariant measures of $\mathbf{f}$ is non-empty and denoted by $M(X, \mathbf{f})$. The attractors of $\mathbf{f}$ will be contained in the support of a special invariant measure called ergodic (see e.g., [61]). These measures can be characterized as follows: for μ-almost all $x \in X$, it is held that

$$\lim_{n\to\infty} \frac{1}{n} \sum_{i=0}^{n-1} \varphi(\mathbf{f}^i(x)) = \int_X \varphi d\mu$$

for any continuous map $\varphi : X \to \mathbb{R}^d$, $d \in \mathbb{N}$. As an application, fixing n big enough, different values of the ergodic average

$$\frac{1}{n} \sum_{i=0}^{n-1} \mathbf{f}^i(x)$$

will indicate the existence of different attractors for a map $\mathbf{f}$ from $X \subset \mathbb{R}^d$ into itself. Here we take as φ the identity on X. Below, we will show an example of how to implement the above idea.

Example 3.9. Now, we consider the γ-Ricker model of order two given by

$$x_{n+1} = a x_n^{\gamma} e^{-(x_n + \rho x_{n-1})},$$

where $a > 1$, $\gamma \geq 1$ and the parameter $\rho \geq 0$ measures the dependence of population of time $n+1$ of the population of time $n-1$. Here, the ergodic averages are useful for finding different attractors in the model. We know that the 1D model can have at most two because the map is unimodal and has negative Schwarzian derivative. Here, we have found parameter values where three attractors are shown. Namely, for $a = 7$, $\gamma = 2.8$ and $\rho = 0.4$ we have found numerical evidences of three attractors; the fixed point 0, a periodic point of period 5 given by $\{1.8798, 1.0562, 1.26931, 2.54529, 4.52122\}$, and an invariant curve shown in Figure 10. In Figure 11, we depict the graph of the ergodic averages for initial conditions on $[0, 10]^2$. The figures indicate the existence of at least three Milnor attractors, but of course, we cannot say whether another attractor may also coexist.

Of course, the above method is not optimal, but it at least makes it possible to identify the different orbits we will use to measure the complexity. The methods explained below are orbit-dependent and borrow ideas from time series analysis (see, eg., [54] or [7]), which allow us to obtain estimations of the topological entropy. Namely, let $\mathcal{S}_m$ be the set of permutations of length m (called embedding dimension) and let $(x_n)_{n=0}^{\infty}$ be a sequence of real numbers. Let $\mathcal{A}_m \subset \mathcal{S}_m$ be the subset of permutations with the property that for any $\pi \in \mathcal{A}_m$ there is $k \in \mathbb{N}$ such that $x_{k+\pi(1)} < x_{k+\pi(2)} < ... < x_{k+\pi(m)}$ and define the permutation entropy of the sequence as

$$h^*((x_n)_{n=0}^{\infty}) = \limsup_{m\to\infty} \frac{1}{m} \log \#\mathcal{A}_m.$$

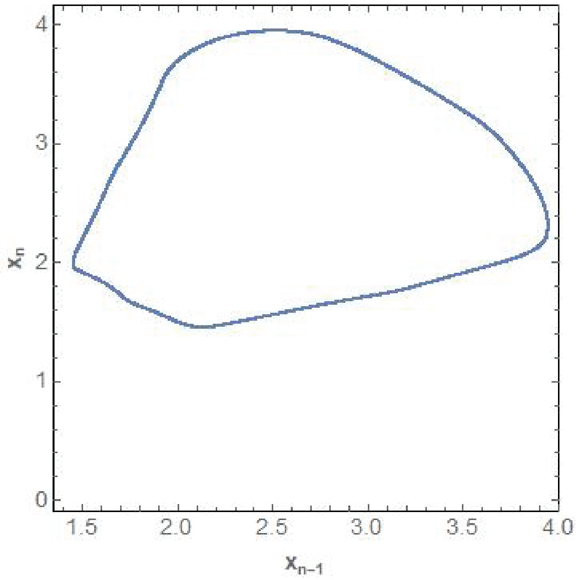

Figure 10. *Fix $a = 7$, $\gamma = 2.8$, $\rho = 0.4$. The invariant curve that seems to be a Milnor attractor.*

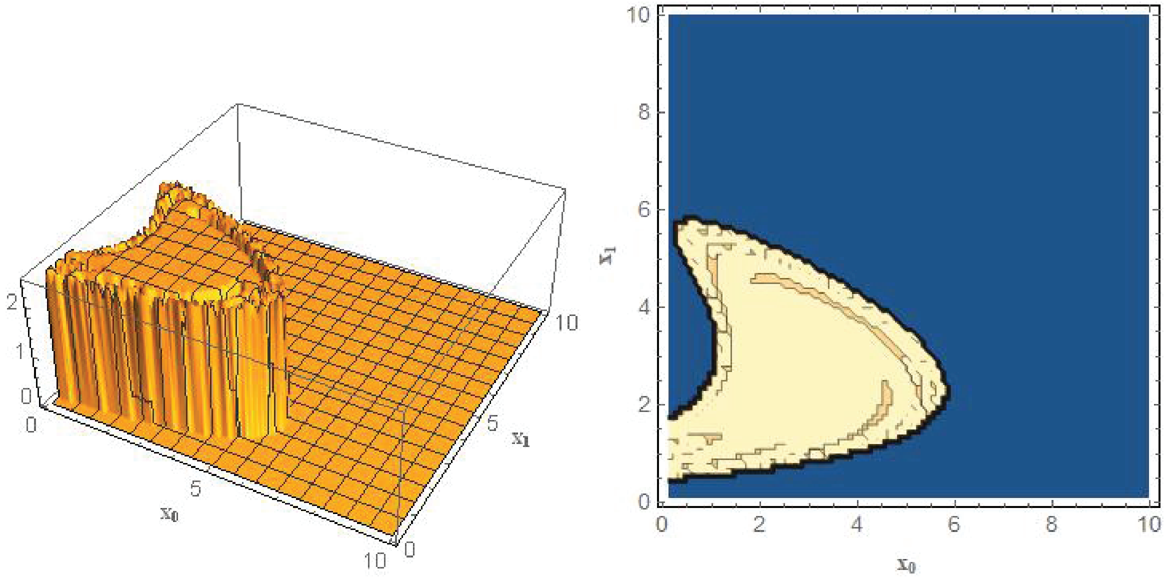

Figure 11. *Fix $a = 7$, $\gamma = 2.8$, $\rho = 0.4$. We depict the ergodic averages when $(x_0, x_1) \in [0, 10]^2$ with step size 0.1.*

Note that we can see easily that $h^*((x_n)_{n=0}^{\infty}) = 0$ if the sequence is periodic or has some monotonicity properties because for any $m \in \mathbb{N}$, the number of elements of $\mathcal{A}_m$ is bounded. The connection between topological entropy and permutation entropy was recently pointed out in [6] by proving the following result. We consider a real map f. For any $\pi \in \mathcal{S}_m$, define the partition $\mathcal{P}_\pi = \{x \in I : f^{\pi(1)}(x) < f^{\pi(2)}(x) < ... < f^{\pi(m)}(x)\}$. Then, if the map f is piecewise monotone (even discontinuous), we have that

$$h(f) = \lim_{n\to\infty} \frac{1}{m} \log \#\{\pi \in \mathcal{S}_m : \mathcal{P}_\pi \neq \emptyset\}.$$

It is just a simple observation that $\mathcal{P}_\pi \neq \emptyset$ provided there is $x \in X$ such that its orbit $\mathrm{Orb}(x, f) = (f^n(x))_{n=0}^{\infty}$ contains a block of length m which can be ordered according to the permutation π. Then, it was proved in [17] the following result.

Theorem 3.10. *Let $f : I \to I$ be continuous and piecewise monotone. Then, for any $y \in I$*

$$h^*(\mathrm{Orb}(y, f)) \leq h(f) = \sup_{x\in I} h^*(\mathrm{Orb}(x, f)).$$

Theorem 3.10 states that the permutation entropy can be used to measure the complexity of dynamical systems. If X is a subset of $\mathbb{R}^d$, $d \in \mathbb{N}$, and we have a model given by $\mathbf{f} : X \to X$, we can consider the natural projections $\pi_i : X \to \mathbb{R}$, and the sequences of real numbers $\pi_i(\mathrm{Orb}(\mathbf{x}, \mathbf{f}))$, for $i = 1, ..., d$ and $\mathbf{x} \in X$. Next, we can compute

$$h_{perm}(\mathrm{Orb}(\mathbf{x}, \mathbf{f})) := \max\{h^*(\pi_i(\mathrm{Orb}(\mathbf{x}, \mathbf{f}))) : i \in \{1, ..., d\}\}$$

as a measure of the complexity of the orbit $\mathrm{Orb}(\mathbf{x}, \mathbf{f})$. Computing $h_{perm}(\mathrm{Orb}(\mathbf{x}, \mathbf{f}))$ for all the different orbits we have classified using the ergodic averages, we obtain a rough measure of the complexity of the system.

Example 3.11. Now, we consider the γ-Ricker model of order two introduced in Example 3.9. In Figure 12, we show the result of computing the permutation entropy for embedding dimension $m = 10$, $a = 10$ and $\rho \in \{0.5, 2.5\}$. We fix a single orbit and depict the bifurcation diagram and the permutation entropy.

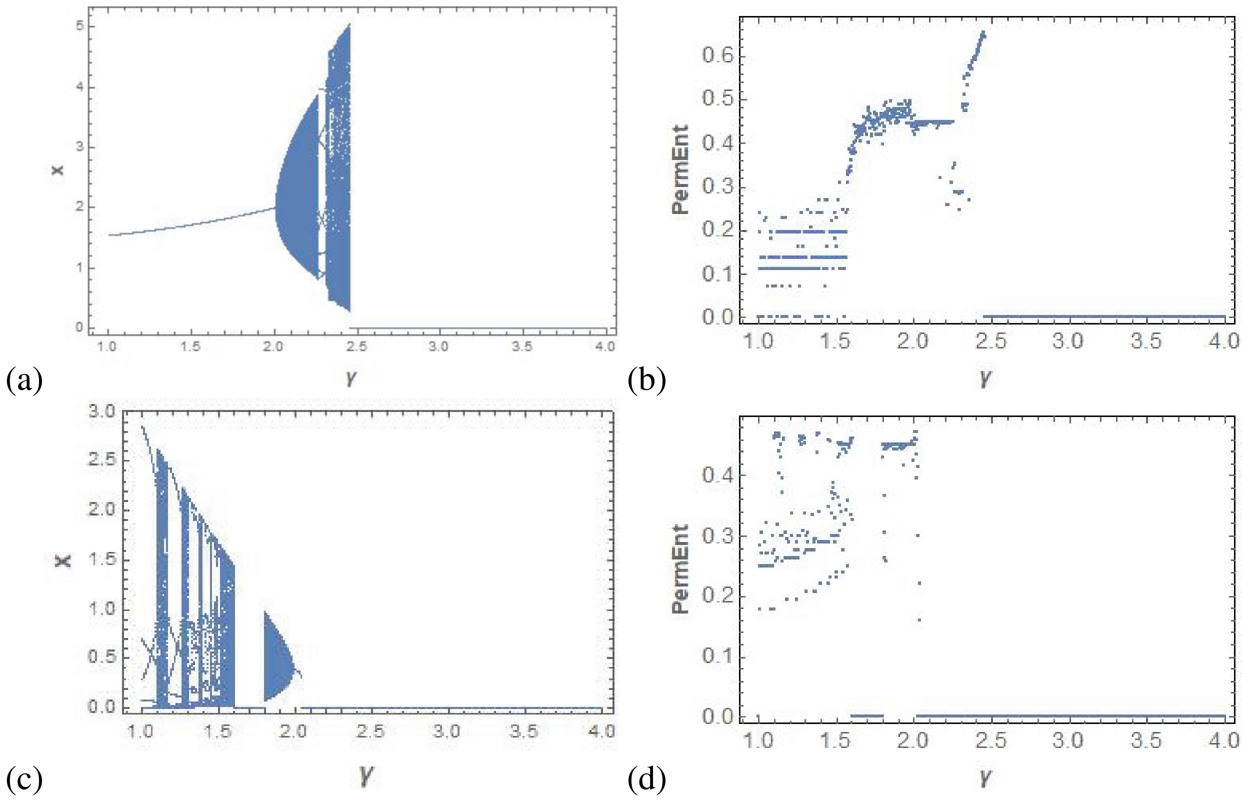

Figure 12. *Fix $a = 10$. Bifurcation diagram for $\rho = 0.5$(a) and 2.5(c) when $\gamma \in (1, 4)$ with step size 0.0025. Topological permutation entropy for $\rho = 0.5$(b) and 2.5(d) of a sample of 10000 points with embedding $m = 10$.*

We can also measure the Lyapunov exponents in those orbits. In this case, given $\mathbf{x} \in X$, they will be given by

$$\mathrm{lex}(\mathbf{x}) = \max\left\{\lim_{n\to\infty} \frac{1}{n} \log |\lambda_i(n)| : i \in \{1, ..., d\}\right\},$$

where $\lambda_i(n)$ is an eigenvalue of $\mathbf{Jf}^n(\mathbf{x})$ (see [47]).

Example 3.12. Now, we consider the γ-Ricker model of order two introduced in 3.9. For the same orbits of Example 3.11 we compute the maximal Lyapunov exponent. The result are shown in Figure 13.

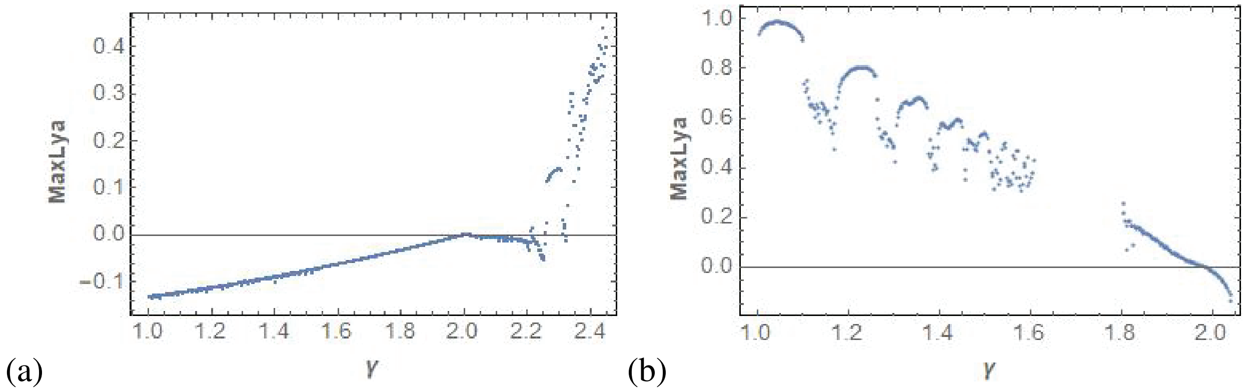

Figure 13. *Fix $a = 10$. Maximal Lyapunov exponent for $\rho = 0.5$(a) and 2.5(c). We take $\gamma \in (1, 4)$ with step size 0.0025, but we do not depict the graph when the population goes to extinction because it is obviously negative since the orbit converges to a LAS fixed point.*

Remark 3.13. *Let us finish this section by noticing that there are another possible instruments to measure complexity that are also orbit-dependent. Among them, we can mention the approximate entropy [48], the sample entropy [50], or the 0-1 test [35]. Since they are orbit dependent, to deal with them one should know how many attractors are in the system. Finding a method to measure complexity that will not be orbit-dependent is a very interesting problem that deserves further investigation.*

Acknowledgements

I wish to thank Habib Marzougui and Dorsaf Bazzaa from the Faculty of Sciences of Bizerte (University of Carthage), who read a preliminary version of this manuscript and suggested interesting improvements. I wish also to thank to the anonymous referee who suggested useful changes to improve the manuscript.

References

[1] R. L. Adler, A. G. Konheim and M. H. McAndrew, *Topological entropy*, Trans. Amer. Math. Soc. 114, (1965) 309-319.

[2] L. Alsedà, J. Llibre, M. Misiurewicz, Combinatorial dynamics and entropy in dimension one, World Scientific Publishing, River Edge, 1993.

[3] Z. AlSharawi, J. S. Cánovas and S. Kallel, *Constrained polynomial roots and a modulated approach to Schur stability*, J. Difference Equ. Appl., (2025), https://doi.org/10.1080/10236198.2025.2455071.

[4] F. Balibrea, V. Jiménez López, *The measure of scrambled sets: a survey*, Acta Univ. M. Belii Ser. Math. 7 (1999), 3-11.

[5] S. Banerjee and R. Parthsarathy, *A q-deformed logistic map and its implications*, J. Phys. A., 44 (2011), 045104.

[6] C. Bandt, G. Keller and B. Pompe, *Entropy of interval maps via permutations*, Nonlinearity 15 (2002), 1595–1602.

[7] C. Bandt and B. Pompe, *Permutation entropy-a natural complexity measure for time series*, Phys. Rev. Lett. 88 (2002), 174102.

[8] J. Banks, J. Brooks, G. Cairns, G. Davis and P. Stacey, *On Devaney's definition of chaos*, Amer. Math. Monthly 99 (1992), 332-334.

[9] R. J. H. Beverton and S. J. Holt, *On the Dynamics of Exploited Fish Populations*, Fishery Investigations Series II Volume XIX, Ministry of Agriculture, Fisheries and Food (1957).

[10] G.I. Bischi, C. Chiarella, M. Kopel and F. Szidarovszky, Nonlinear oligopolies, Springer Verlag (2010).

[11] G.I. Bischi and L. Cerboni Baiardi, *Fallacies of composition in nonlinear marketing models*, Communications in Nonlinear Science and Numerical Simulation. 20 (2015) 209–228.

[12] L.S. Block and W.A. Coppel, Dynamics in one dimension, Lecture Note in Mathematics 1513, Springer-Verlag, Berlin, 1992.

[13] L. Block, J. Keesling, S. H. Li and K. Peterson, *An improved algorithm for computing topological entropy*, J. Stat. Phys. 55 (1989), 929–939.

[14] L. Block and J. Keesling, *Computing the topological entropy of maps of the interval with three monotone pieces*, J. Statist. Phys. 66 (1992) 755-774.

[15] R. Bowen, *Entropy for group endomorphism and homogeneous spaces*, Trans. Amer. Math. Soc. 153 (1971), 401-414.

[16] J. S. Cánovas, *Reducing competitors in a Cournot-Theocharis oligopoly model*, Journal of Difference Equations and Applications, 15, (2009) 153-165.

[17] J. S. Cánovas, *Estimating topological entropy from individual orbits*, International Journal of Computer Mathematics 86 (2009), 1901-1906.

[18] J. S. Cánovas, *On q-deformed logistic maps*, Discrete. continuous Dyn sys-B., 27(5) (2022), 2833.

[19] J. S. Cánovas, *On the delayed Cournot-Theocharis oligopoly model under adaptive expectations*, Communications in Nonlinear Science and Numerical Simulation 117 (2023) 106981.

[20] J. S. Cánovas and M. Muñoz, *Revisiting Parrondo's paradox for the logistic family*, Fluct. Noise Lett., 12 (2013), 1350015.

[21] J. S. Cánovas and M. Muñoz-Guillermo, *Computing topological entropy for periodic sequences of unimodal maps*, Comm. in Nonlinear Science and Numerical Simulation, 19, (2014) 3119-3127.

[22] J. S. Cánovas and M. Muñoz-Guillermo, *Computing the topological entropy of continuous maps with at most three different kneading sequences with applications to Parrondo's paradox*, Chaos, Solitons & Fractals, 83, (2016) 1-17.

[23] J. S. Cánovas and M. Muñoz-Guillermo, *On the complexity of economic dynamics: An approach through topological entropy*, Chaos, Solitons & Fractals, 103, (2017) 163-176.

[24] J. Cánovas and M. Muñoz, *On the dynamics of the q-deformed logistic map*, Phys. Lett. A, 383 (2019), 1742-1754.

[25] J. S. Cánovas, M. Ruiz and T. Puu, *The Cournot-Theocharis problem reconsidered*, Chaos, Solitons & Fractals, 37 (2008), 1025-1039.

[26] W. de Melo and S. van Strien, One-dimensional dynamics, Springer Verlag, New York (1993).

[27] R.L. Devaney, An introduction to chaotic dynamical systems, Addison-Wesley, Redwood City (1989).

[28] B. S. Du, *A simple proof of Sharkovsky's theorem*, Amer. Math. Monthly 111 (2004), 595-599.

[29] S. N. Elaydi, Discrete Chaos: With Applications in Science and Engineering (2nd ed.). Chapman and Hall/CRC 2007.

[30] H. A. El-Morshedy and E. Liz, *Globally attracting fixed points in higher order discrete population models*, J. Math. Biol., 53 (2006), 365-384.

[31] H. A. El-Morshedy and V. Jiménez L'opez, *Global attractors for difference equations dominated by one-dimensional maps*, J. Difference Equ. Appl., 14 (2008), 391-410.

[32] R. W. Farebrother, *Simplified samuelson conditions for cubic and quartic equations*, The Manchester School, 41 (1973), 396-400.

[33] R. W. Farebrother, *Simplified samuelson conditions for quintic equations*, The Manchester School, 42 (1974), 279-282.

[34] V. V. Fedorenko, A. N. Sharkovsky and J. Smítal, *Characterizations of weakly chaotic maps of the interval*, Proc. Amer. Math. Soc. 110 (1990), 141–148.

[35] G. A. Gottwald and I. Melbourne, *The 0-1 Test for Chaos: A Review*. In: Skokos, C., Gottwald, G., Laskar, J. (eds) Chaos Detection and Predictability. Lecture Notes in Physics, vol 915. Springer, Berlin, Heidelberg (2016).

[36] J. Guckhenheimer, *Sensitive Dependence to Initial Conditions for one-dimensional maps*, Comm. Math. Phys. 70 (1979), 133-160.

[37] R. Jaganathan and S. Sinha, *A q-deformed nonlinear map*, Phys. Lett. A., 338 (2005), 277-287.

[38] E. I. Jury, *On the roots of a real polynomial inside the unit circle and a stability criterion for linear discrete systems*, IFAC Proc. 1 (1963), 142-153.

[39] M. Kopel, *Simple and complex adjustment dynamics in Cournot duopoly models*, Chaos, Solitons & Fractals 7 (1996), 2031-2048.

[40] Y. A. Kuznetsov, Elements of applied bifurcation theory, Springer-Verlag, New York, 2004.

[41] Y. A. Kuznetsov and H. G. E. Meijer, *Numerical Normal Forms for Codim 2 Bifurcations of fixed points with at most two critical eigenvalues*, SIAM Journal on Scientific Computing 26 (2005), 1932-1954.

[42] G. Ladas and V.L. Kocic. Global behavior of nonlinear difference equations of higher order with applications, volume 256. World Scientific Publishing Co., Inc., River Edge, NJ, first edition, 1993.

[43] T. Y. Li and J. A. Yorke, *Period three implies chaos*, Amer. Math. Monthly 82 (1975), 985–992.

[44] Liz, E., *A Global Picture of the Gamma-Ricker Map: A Flexible Discrete-Time Model with Factors of Positive and Negative Density Dependence*, Bull. Math. Biol. 80 (2018) 417-434.

[45] R. M. May, *Simple mathematical models with very complicated dynamics*, Nature 261 (1976), 459-467.

[46] J. Milnor, *On the concept of attractor*, Communications in Mathematical Physics, Comm. Math. Phys. 99 (1985) 177-195.

[47] V.I. Oseledets, *A multiplicative ergodic theorem. Lyapunov characteristic numbers for dynamical systems*, Trans. Moscow Math. Soc. 19 (1968), 197-231. Moscov.Mat.Obsch.19 (1968), 179-210.

[48] S. M. Pincus, *Approximate entropy as a measure of system complexity*, Proc. Natl. Acad. Sci. 88 (1991), 2297-2301.

[49] T. Puu, *Chaos in duopoly pricing*, Chaos, Solitons & Fractals, 1 (1991), 573-581.

[50] J. S. Richman and J. R. Moorman, *Physiological time-series analysis using approximate entropy and sample entropy*, Am J Physiol Heart Circ Physiol, 278 (2000), H2039-H2049.

[51] W. E. Ricker, *Stock and Recruitment*, Journal of the Fisheries Board of Canada, 11 (1954) 559-623.

[52] A.N. Sharkovsky, *Coexistence of cycles of a continuous transformation of a line into itself*, Ukrain. Mat. Zh. 16 (1964), 61-71 (in Russian).

[53] D. Singer, *Stable Orbits and Bifurcation of Maps of the Interval*, SIAM Journal on Applied Mathematics, 35 (1978) 260-267.

[54] M. Small, Applied nonlinear time series analysis. Applications in physics, physiology and finance, World Scientific Series on Nonlinear Science. Series A: Monographs and Treatises, 52. World Scientific Publishing Co. Pte. Ltd., Hackensack, NJ, 2005.

[55] J. Smítal, *Chaotic functions with zero topological entropy*, Trans. Amer. Math. Soc. 297 (1986), 269-282.

[56] S. Smale, *Differentiable dynamical systems*, Bull. Amer. Math. Soc. 73 (1967), 747-817.

[57] R. D. Theocharis, *On the stability of the Cournot solution on the oligopoly problem*, Review of Economic Studies, 27 (1960), 133-134.

[58] H. Thunberg, *Periodicity versus chaos in one–dimensional dynamics*, SIAM Review 43 (2001), 3-30.

[59] C. Tsallis, *Nonextensive statistical mechanics: a brief review of its present status*, An. Acad. Bras. Cienc., 74 (2002), 393-414.

[60] S. van Strien and E. Vargas, *Real bounds, ergodicity and negative Schwarzian for multimodal maps*, J. Amer. Math. Soc. 17 (2004), 749-782.

[61] P. Walters, An introduction to ergodic theory, Springer Verlag, New York (1982).

[62] D. Whitley, *Discrete dynamical systems in dimensions one and two*, Bull. London Math. Soc. 15 (1983), 177-217.

[63] E. M. Wright, *Solution of the Equation* $ze^z = a$, Bull. Amer. Math. Soc. 65 (1959), 89-93.